

## In a Clean High- $T_c$ Superconductor You Do Not See the Gap

K. Kamarás,<sup>(a)</sup> S. L. Herr, C. D. Porter, N. Tache, and D. B. Tanner

*Department of Physics, University of Florida, Gainesville, Florida 32611*

S. Etemad, T. Venkatesan, and E. Chase

*Bell Communications Research, Red Bank, New Jersey 07701*

A. Inam, X. D. Wu, M. S. Hegde, and B. Dutta<sup>(b)</sup>

*Department of Physics, Rutgers University, Piscataway, New Jersey 08855*

(Received 5 June 1989)

The frequency-dependent conductivity of laser-deposited  $\text{YBa}_2\text{Cu}_3\text{O}_{7-\delta}$  thin films shows an onset of midinfrared absorption at  $\sim 140\text{ cm}^{-1}$  and structure in the  $400\text{--}500\text{-cm}^{-1}$  region. These low-energy absorptions occur both above and below  $T_c$ , making them unlikely to be the superconducting gap in the usual BCS sense. The absorption across the gap is weak because the high- $T_c$  materials are in the clean limit; this weak absorption is masked by the midinfrared absorption.

PACS numbers: 78.30.Er, 74.70.Vy, 78.20.Ci

Most studies of the infrared properties of high- $T_c$  superconductors<sup>1</sup> have focused on the superconducting energy gap and the nature of the strong midinfrared absorption. In *ab*-plane-oriented material two spectral features have been assigned to the superconducting gap. One<sup>2,3</sup> is an absorption onset at  $\sim 140\text{ cm}^{-1}$ , below which the superconducting-state reflectance  $\mathcal{R}_s$  is (within experimental error) 100%. This frequency corresponds to  $(3.1\text{--}3.2)k_B T_c$  for the reduced- $T_c$  samples of Ref. 2 and  $2.1k_B T_c$  for the  $T_c = 91\text{ K}$  samples of Ref. 3. The other<sup>3,4</sup> is a shoulder in the superconducting-state reflectance  $\mathcal{R}_s$  (at  $440\text{ cm}^{-1}$  in  $\text{YBa}_2\text{Cu}_3\text{O}_{7-\delta}$ ). When the ratio of superconducting to normal-state reflectance,  $\mathcal{R}_s/\mathcal{R}_n$ , is measured,<sup>4</sup> this shoulder becomes a maximum at  $460\text{--}480\text{ cm}^{-1}$ , or  $7.3k_B T_c$  when  $T_c = 92\text{ K}$ .

The normal-state infrared properties have also received various interpretations. Early discussions of crystals of films—largely at room temperature—used a Drude model with a constant, very short, relaxation time.<sup>4–6</sup> Because this simple model fails to account for the temperature dependence of the infrared properties,<sup>2,7</sup> either a generalized Drude model, with a strongly frequency-dependent relaxation rate and effective mass,<sup>2,8</sup> or a model of parallel conduction by several types of carriers having differing concentrations and relaxation rates<sup>3</sup> has been used in recent analyses. A fourth picture attributes most of the midinfrared absorption to a direct electronic excitation.<sup>9–14</sup>

In this paper we discuss the infrared reflectance of epitaxially grown laser-deposited films of  $\text{YBa}_2\text{Cu}_3\text{O}_{7-\delta}$ . We conclude that neither the absorption onset at  $140\text{ cm}^{-1}$  nor the structure at  $440\text{--}480\text{ cm}^{-1}$  should be assigned to the superconducting gap. Both are present in the normal-state data at essentially the same frequencies. Furthermore, we demonstrate that the clean limit holds,<sup>12</sup> making the gap difficult to see by infrared absorption.

Our films were made by pulsed-eximer-laser (248 nm, 30 ns) deposition<sup>15</sup> from a composite  $\text{YBa}_2\text{Cu}_3\text{O}_{7-\delta}$  tar-

get onto  $700\text{--}750^\circ\text{C}$   $\text{SrTiO}_3$  substrates. An oxygen background pressure of 200 mTorr was maintained during the deposition. Three films, thicknesses between 2000 and 5000 Å, have been measured. The highly oriented films are extremely smooth and have the *c* axis normal to the surface; helium-ion-channeling experiments, which observe less than 3% scattering, indicate that the *ab*-plane orientation is as good as in crystals. The normal-state resistivity is linear, with an extrapolated zero-temperature intercept of  $0 \pm 2\ \mu\Omega\text{ cm}$ . The films are superconducting with  $T_c$  of 89–91 K, depending on sample, and  $\Delta T_c \approx 0.2\text{ K}$ .

Reflectance measurements were made with a Bruker interferometric superconductor over  $50\text{--}5000\text{ cm}^{-1}$  (0.0062–0.62 eV) and with a grating monochromator over  $1000\text{--}32000\text{ cm}^{-1}$  (0.12–4 eV). The 300-K reflectance was measured relative to an Al reference and corrected for the known reflectance of the Al. Because of the high quality of the surfaces there was no need to coat the samples with a metal to estimate the scattering losses. A continuous-flow cryostat was used to cool the sample to temperatures down to 20 K. The temperature-dependent reflectance was measured relative to the 300-K reflectance.

The low-frequency reflectance of two samples is shown in Fig. 1. The upper panel shows a film with  $T_c = 91\text{ K}$ ; the lower one with  $T_c = 89\text{ K}$ . To within experimental error of  $\pm 0.5\%$ , the low-temperature  $\mathcal{R}_s$  is unity up to  $\approx 140\text{ cm}^{-1}$  in both samples; above this frequency  $\mathcal{R}_s$  falls off slowly, with a pronounced shoulder at  $440\text{ cm}^{-1}$  and a broad reflectance edge in the near infrared.<sup>2,3,8,12</sup> The reflectance was essentially temperature independent below  $\sim 60\text{ K}$ ; above this temperature decreased reflectance was observed at all frequencies.

From the reflectance we determined the frequency-dependent conductivity  $\sigma_1(\omega)$  and real dielectric function  $\epsilon_1(\omega)$  using Kramers-Kronig analysis. The Kramers-Kronig procedure has trouble where  $\mathcal{R}_s$  is unity  $\pm$  noise: as  $\mathcal{R} \rightarrow 1$ , the signal is not  $\mathcal{R}$  but  $1 - \mathcal{R}$ , making

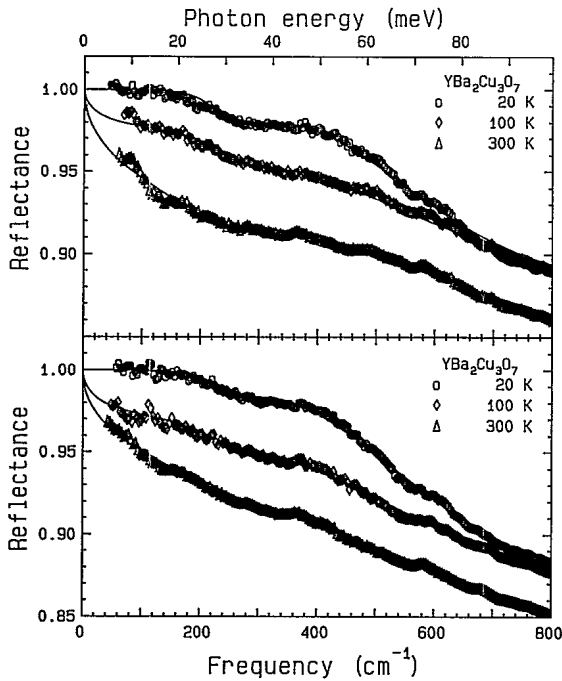


FIG. 1. Measured far-infrared reflectance of two  $\text{YBa}_2\text{Cu}_3\text{O}_{7-s}$  films at 20, 100, and 300 K. The results from fits with a sum of Drude ( $D$ ) and Lorentzian ( $L$ ) terms are shown as lines. The Drude parameters (in  $\text{cm}^{-1}$ ) are as follows: (upper panel) 300 K,  $\omega_{pD}=7800$  and  $1/\tau=280$ ; 100 K,  $\omega_{pD}=8800$  and  $1/\tau=80$ ; 20 K,  $\omega_{pD}=9100$  and  $1/\tau=0$ ; (lower panel) 300 K,  $\omega_{pD}=7500$  and  $1/\tau=220$ ; 100 K,  $\omega_{pD}=8200$  and  $1/\tau=110$ ; 20 K,  $\omega_{pD}=8400$  and  $1/\tau=0$ . The Lorentzian parameters  $\omega_{el}$ ,  $\omega_{pl}$ ,  $\gamma_l$  are as follows:  $L_1$ , 300, 3000, 210;  $L_2$ , 740, 9900, 1600;  $L_3$ , 3300, 14600, 7800.

the signal-to-noise ratio zero when  $\mathcal{R}=1$ . To avoid this, we have adopted as an extrapolation procedure setting  $\mathcal{R}=1.0$  when the measured reflectance reaches unity. This gives a phase shift of  $-\pi$  and a pure real dielectric function.

Figure 2 shows  $\sigma_1(\omega)$  at four temperatures for our  $T_c=91$  K sample. Above  $T_c$  a narrow low-frequency peak exists whose intercept agrees with dc measurements. There is weak structure in the 200–600- $\text{cm}^{-1}$  region while at higher frequencies there is a broad, nearly temperature-independent conductivity. Below  $T_c$  the low-frequency upturn is gone; the conductivity shows a strong onset at 120–140  $\text{cm}^{-1}$  (corresponding to the frequency where  $\mathcal{R}_s$  falls below unity) with a maximum around 280  $\text{cm}^{-1}$ , a minimum at 430  $\text{cm}^{-1}$ , and a second broad maximum near 800  $\text{cm}^{-1}$ . Both the 140- $\text{cm}^{-1}$  onset<sup>2,3</sup> and the 430- $\text{cm}^{-1}$  minimum<sup>3,4</sup> have been assigned to the superconducting gap. However, we cannot support either assignment, because the same features are present in our normal-state data. They are seen in Figs. 1 and 2 as weak structure on the Drude background but much more clearly in Fig. 3, which shows  $\sigma_1(\omega)$  with the Drude contribution subtracted.

We obtained the curves in Fig. 3 in the following way. We made a least-squares fit of  $\mathcal{R}_n$  with a model dielec-

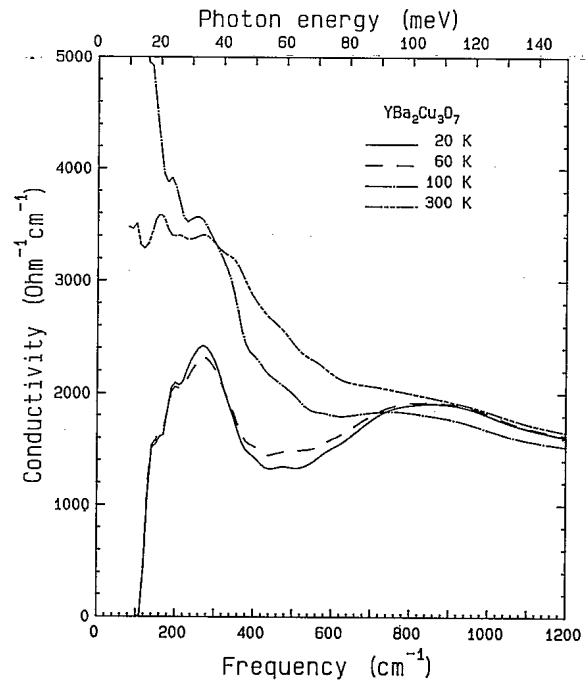


FIG. 2. Frequency-dependent conductivity of a  $T_c=91$  K film of  $\text{YBa}_2\text{Cu}_3\text{O}_{7-s}$  at 20, 60, 100, and 300 K.

tric function which consisted of a Drude part and several Lorentzian contributions. These fits are shown in Fig. 1 as solid lines. The Drude part represents the contribution of free carriers while the Lorentzians are means to represent excitations of bound electrons, interband transitions, etc. The total dielectric function is

$$\epsilon(\omega) = -\frac{\omega_{pD}^2}{\omega^2 + i\omega/\tau} + \sum_{l=1}^3 \frac{\omega_{pl}^2}{\omega_{el}^2 - \omega^2 - i\omega\gamma_l} + \epsilon_\infty, \quad (1)$$

where  $\omega_{pD}$  and  $1/\tau$  are the plasma frequency and relaxation rate of the Drude carriers, while  $\omega_{el}$ ,  $\omega_{pl}$ , and  $\gamma_l$  are the center frequency, strength, and width of the  $l$ th

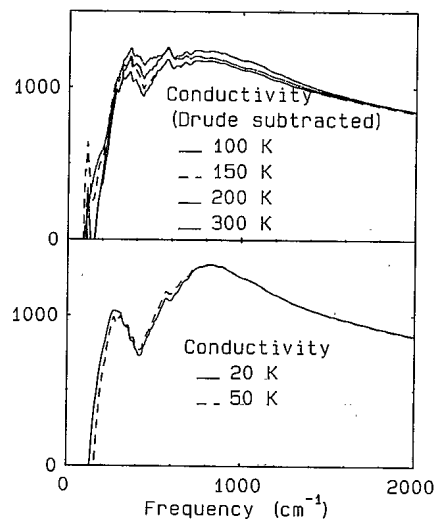


FIG. 3. Upper panel: Frequency-dependent conductivity of a  $T_c=89$  K film above  $T_c$ , with the Drude contribution subtracted. Lower panel: Conductivity below  $T_c$ .

Lorentzian contribution. For the fits below  $T_c$  we collapsed the Drude term to a  $\delta$  function but kept the remaining terms unchanged.

To fit the broad-band midinfrared absorption requires three components, at 300, 740, and 3300  $\text{cm}^{-1}$ . Higher-frequency electronic excitations, previously seen by ellipsometry,<sup>16</sup> are here lumped into  $\epsilon_\infty$ . In the fit, the wings of the first two Lorentzian terms are broader than the structure in  $\sigma_1(\omega)$ , indicating that these are not particularly good model dielectric functions. [It has recently been shown<sup>17</sup> that a simple model of strong coupling between the bound carriers and a phonon in the 52-meV (430- $\text{cm}^{-1}$ ) range can give the observed antiresonance structure in  $\sigma_1(\omega)$ . This electron-phonon model replaces the two Lorentzian terms at 300 and 740  $\text{cm}^{-1}$  with a single band at 400  $\text{cm}^{-1}$  linearly coupled to a phonon at 433  $\text{cm}^{-1}$ .]

The curves in the upper part of Fig. 3 were obtained by subtracting the Drude part of  $\sigma_1(\omega)$  for our  $T_c = 89$ -K sample, using the parameters from the reflectance fit. The result for our  $T_c = 91$  K sample would be similar, except for a larger low-frequency  $\sigma_1(\omega)$ . In Fig. 3 it can be seen that without the free-carrier contribution, the normal-state  $\sigma_1(\omega)$  has the same form as the superconducting state  $\sigma_1(\omega)$ : an onset near 140  $\text{cm}^{-1}$ , a maximum around 350  $\text{cm}^{-1}$ , a minimum at 430  $\text{cm}^{-1}$ , and a second broad maximum near 750  $\text{cm}^{-1}$ . With decreasing temperature the 430- $\text{cm}^{-1}$  minimum grows deeper and the 140- $\text{cm}^{-1}$  edge becomes a bit steeper; this trend continues below  $T_c$ . Because the 140- $\text{cm}^{-1}$  onset is present in the normal state up to 300 K it is unlikely to be the superconducting gap. Similarly, there is no obvious absorption feature in the 400-500- $\text{cm}^{-1}$  region below  $T_c$  which is absent above  $T_c$ . (In fact, the shoulder in the reflectance which has been the principal evidence used<sup>4</sup> in support of a 480- $\text{cm}^{-1}$  gap is quite evident in normal-state data.<sup>2,3,12-14</sup>)

There are two other reasons why we suspect that neither feature is the superconducting gap. First, both occur at nearly the same energy in reduced- $T_c$  crystals<sup>2</sup> and  $T_c \approx 91$  K films, both those reported here and elsewhere,<sup>3</sup> and thus do not scale with  $T_c$ . Second, a nearly identical conductivity spectrum occurs<sup>13</sup> in  $T_c \approx 85$  K crystals of  $\text{Bi}_2\text{Sr}_2\text{CaCu}_2\text{O}_8$ , with the exception that the onset for  $T < T_c$  occurs at 300  $\text{cm}^{-1}$  and the first minimum is at  $\sim 500$   $\text{cm}^{-1}$ . The presence in the normal state of this absorption is clearly seen in  $\mathcal{R}_n$  and in  $\sigma_1(\omega)$  above  $T_c$  (see Fig. 4 of Ref. 13). If the onset in these materials were the gap, one would have  $2\Delta/k_B T_c \approx 2.2$  in films,  $2\Delta/k_B T_c \approx 3.1-3.2$  in O-deficient crystals, and  $2\Delta/k_B T_c = 5.1$  in  $\text{Bi}_2\text{Sr}_2\text{CaCu}_2\text{O}_8$ . An alternative interpretation is that the onset is a direct electronic absorption, whose energy is determined by the material.

Why is absorption across the superconducting gap not seen? In our view, this is because  $\text{YBa}_2\text{Cu}_3\text{O}_{7-\delta}$  is in the clean limit, normal skin effect regime of supercon-

ductivity<sup>12</sup> ( $1/\tau \ll 2\Delta$ ;  $\xi_0 \ll l \ll \lambda_L$ ). The parameters of the fits to  $\mathcal{R}_n$  support this view. At  $T = 100$  K we find  $\omega_{pD} = 8800$  and  $1/\tau = 100$   $\text{cm}^{-1}$  for the  $T_c = 91$  K film and  $\omega_{pD} = 8200$  and  $1/\tau = 110$   $\text{cm}^{-1}$  for the  $T_c = 89$  K film. The plasma frequency is weakly  $T$  dependent while the scattering rate is essentially  $T$  linear (like the resistivity) with zero intercept:

$$\frac{1}{\tau} \approx (100 \text{ cm}^{-1}) \frac{T}{100 \text{ K}} \quad (2)$$

The 100-K value corresponds to  $\tau = 5.3 \times 10^{-14}$  sec and (if  $v_F = 3 \times 10^7$  cm/sec) a mean free path of  $l = 160$  Å. Thus at 100 K,  $1/\tau \sim 1.4 k_B T_c$ , which is definitely smaller than the BCS gap value of  $3.5 k_B T_c$ . At 20 K, we expect a still smaller value of  $1/\tau$  and a stronger inequality.

According to the clean-limit picture,<sup>18</sup> all of the oscillator strength of the Drude conductivity appears under the zero-frequency  $\delta$  function in  $\sigma_{1S}$ ; none is left for transitions across the superconducting gap.<sup>19</sup> Then, the real part of the dielectric function at low frequencies is<sup>1</sup>

$$\epsilon_1(\omega) = \epsilon_{1b} - \frac{\omega_{pS}^2}{\omega^2}, \quad (3)$$

where  $\epsilon_{1b}$  is the bound-electron contribution to  $\epsilon_1(\omega)$  [i.e., the zero-frequency sum of all the Lorentzians in Eq. (1)] and  $\omega_{pS}$ , the plasma frequency of the superconducting charge carriers, equals the Drude plasma frequency. Figure 4 shows the real dielectric function of our  $T_c = 91$  K film, plotted against  $\omega^{-2}$ . Below 50 K  $\epsilon_1(\omega)$ , a straight line over most of the range, satisfies Eq. (3). We find  $\omega_{pS} = 9000 \pm 400$   $\text{cm}^{-1}$ , very close to the normal-state fitted result at 100 K for this film of  $\omega_{pD} \approx 8800$   $\text{cm}^{-1}$ . Confidence in the correctness of the clean-limit picture is *a posteriori* based on the agreement between the superconducting and normal-state determinations of the plasma frequency.

We note that the slope of  $\epsilon_1(\omega)$  vs  $\omega^{-2}$  is essentially a direct measurement of the London penetration depth,  $\lambda_L = 1/2\pi\omega_{pS}$  ( $\omega_{pS}$  in  $\text{cm}^{-1}$ ); we obtain  $\lambda_L = 1750 \pm 100$  Å. This value, which is less than the film thickness, is somewhat larger than the 1400-Å *ab*-plane  $\lambda_L$  found

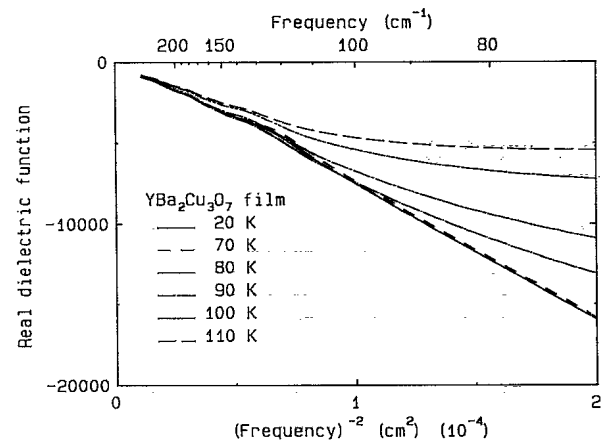


FIG. 4. Real part of the dielectric function, plotted against  $\omega^{-2}$ . The range of the data shown is 300-70  $\text{cm}^{-1}$ .

from muon-spin-rotation measurements<sup>20</sup> in  $\delta=0$  samples. Some—but probably not all—of the difference between the two measurements might be attributed to slightly lower oxygen content in the films.

We turn now to the midinfrared absorption in these materials, which has been variously attributed to a strongly frequency-dependent scattering,<sup>2,8</sup> to parallel conduction by several types of conduction electrons having differing concentrations and relaxation rates,<sup>3</sup> and to a direct electronic excitation.<sup>9–13</sup> Frequency-dependent scattering can be due to a Holstein<sup>21</sup> process, in which an electron absorbs a photon of energy  $\hbar\omega$ , emits some excitation at  $\hbar\Omega$ , and scatters. To conserve energy, one must have  $\hbar\omega > \hbar\Omega$ . By assuming a narrow band of excitations in the 250–500-cm<sup>-1</sup> range strongly coupled ( $\lambda \approx 3-9$ ) to the conduction electrons, the strongly temperature-dependent far-infrared behavior and the temperature-independent midinfrared absorption can be described within a Holstein picture.<sup>2,8</sup> No direct midinfrared absorption is included in these models.

Two factors argue against this picture. First, strong coupling to the excitations leads to a pronounced deviation from a  $T$ -linear dc resistance, in disagreement with experiment.<sup>14,22,23</sup> The  $T$ -linear resistivity is consistent with a weak coupling to low-energy ( $\hbar\Omega \ll 60$  cm<sup>-1</sup>) excitations. Using  $1/\tau = 2\pi k_B T$ , our fitted  $1/\tau$  implies  $\lambda = 0.2$ . This in turn leads to a weak frequency dependence in  $\sigma_1(\omega)$  at  $\omega \sim \Omega$ , but this is smaller than the deviations from Drude behavior shown in Figs. 2 and 3. Second, if there is a superconducting gap then the Holstein process requires that the photon energy provide both the gap energy  $2\Delta$  and the energy of the emitted excitation  $\hbar\Omega$ , causing a shift of the Holstein structure in  $\sigma_1(\omega)$  to higher frequencies below  $T_c$ . However, there is no feature in Figs. 1–3 which shifts to higher frequencies below  $T_c$ .

The  $T$ -linear resistivity also rules out several parallel conduction channels.<sup>3</sup> If there were temperature-independent conduction in parallel with temperature-dependent conduction, the resistivity would show signs of saturation at high temperatures.

Our data support the idea that the midinfrared absorption is a direct electronic excitation. Earlier we had suggested a (Frenkel) exciton,<sup>10</sup> but other possibilities obviously exist.<sup>24,25</sup>

In conclusion, we make the following points: (1) Although plausible arguments have been made for superconducting gaps in YBa<sub>2</sub>Cu<sub>3</sub>O<sub>7- $\delta$</sub>  at 140 cm<sup>-1</sup> and at 480 cm<sup>-1</sup>, neither of these features is the gap since they are seen in the normal state. (2) These features become more visible below  $T_c$  because the Drude free carriers have condensed. (3) The high- $T_c$  superconductors are clean-limit superconductors, with essentially all of the conduction-electron oscillator strength under the zero-frequency  $\delta$  function. (4) The midinfrared absorption is a direct electronic absorption, with an onset at 140 cm<sup>-1</sup> in YBa<sub>2</sub>Cu<sub>3</sub>O<sub>7- $\delta$</sub>  and 300 cm<sup>-1</sup> in Bi<sub>2</sub>Sr<sub>2</sub>CaCu<sub>2</sub>O<sub>8</sub>, indi-

cating a complex low-energy excitation spectrum in these materials.

The work at Florida was supported by U.S. Defense Advanced Research Projects Agency through Contract No. MDA972-88-J-1006.

(a)Permanent address: Central Research Institute for Physics, Budapest, Hungary.

(b)Permanent address: Physics Department, Middlebury College, Middlebury, VT 05753.

<sup>1</sup>For a review of work up to October 1988, see Thomas Timusk and David B. Tanner, in *Physical Properties of High Temperature Superconductors I*, edited by Donald M. Ginsberg, (World Scientific, Singapore, 1989), p. 339.

<sup>2</sup>G. A. Thomas *et al.*, Phys. Rev. Lett. **61**, 1313 (1988).

<sup>3</sup>J. Schützmann *et al.*, Europhys. Lett. **8**, 679 (1989); U. Hoffmann *et al.*, Solid State Commun. **70**, 325 (1989).

<sup>4</sup>Z. Schlesinger *et al.*, Phys. Rev. Lett. **59**, 1958 (1987); R. T. Collins *et al.*, Phys. Rev. Lett. **63**, 422 (1989).

<sup>5</sup>I. Bozovic *et al.*, Phys. Rev. Lett. **59**, 2219 (1987).

<sup>6</sup>G. A. Thomas *et al.*, Jpn. J. Appl. Phys. Suppl. **26**, 2044 (1987); J. Orenstein and D. H. Rapkine, Phys. Rev. Lett. **60**, 968 (1988).

<sup>7</sup>K. Kamarás *et al.*, Phys. Rev. Lett. **60**, 969 (1988); D. B. Tanner *et al.*, Synth. Met. **29**, F715 (1989).

<sup>8</sup>R. T. Collins *et al.*, Phys. Rev. B **39**, 6571 (1989).

<sup>9</sup>S. L. Herr *et al.*, Phys. Rev. B **36**, 733 (1987).

<sup>10</sup>K. Kamarás *et al.*, Phys. Rev. Lett. **59**, 919 (1987).

<sup>11</sup>D. A. Bonn *et al.*, Phys. Rev. B **37**, 1547 (1988).

<sup>12</sup>T. Timusk *et al.*, Phys. Rev. B **38**, 6683 (1988).

<sup>13</sup>M. Reedyk *et al.*, Phys. Rev. B **38**, 11981 (1988).

<sup>14</sup>S. L. Cooper *et al.* (to be published); Joseph Orenstein *et al.* (to be published).

<sup>15</sup>A. Inam *et al.*, Appl. Phys. Lett. **51**, 1112 (1989).

<sup>16</sup>M. K. Kelly *et al.*, Phys. Rev. B **38**, 870 (1988).

<sup>17</sup>T. Timusk and D. Tanner (to be published).

<sup>18</sup>The clean-limit or plasmon model is *not* a zero-gap model. Instead, it is analogous to a London or infinite-gap model. Thus when the authors of Ref. 12 state that the gap cannot be seen by infrared means, they do not mean that  $2\Delta=0$ . In fact, for the model to hold one must have  $2\Delta \gg 1/\tau$ .

<sup>19</sup>S. Strässler and K. Fulde (unpublished); see M. Tinkham, in *Far Infrared Properties of Solids*, edited by S. S. Mitra and S. Nudelman (Plenum, New York, 1974), p. 431. For frequencies just above  $2\Delta$ , the clean-limit  $\sigma_{1s}(\omega)$  exceeds  $\sigma_{1n}(\omega)$  by about a factor of 2, but  $\sigma_{1n}$  is reduced from its dc value by a factor of  $(2\Delta\tau)^2 \gg 1$ .

<sup>20</sup>D. R. Harshman *et al.*, Phys. Rev. B **39**, 851 (1989).

<sup>21</sup>T. Holstein, Phys. Rev. **96**, 539 (1954); Ann. Phys. (N.Y.) **29**, 410 (1964).

<sup>22</sup>Following P. B. Allen and R. Silbergliitt, Phys. Rev. B **9**, 4733 (1974), and assuming a 250-cm<sup>-1</sup>  $\delta$  function for  $a^2F(\omega)$ , this calculation finds a drop below a  $T$ -linear (with zero intercept) scattering rate at and below 300 K.

<sup>23</sup>M. Gurvitch and A. T. Fiory, Phys. Rev. Lett. **59**, 1337 (1987).

<sup>24</sup>M. J. Rice, Y. R. Wang, and E. J. Mele, Phys. Rev. B **40**, 5304 (1989).

<sup>25</sup>C. M. Varma *et al.*, Phys. Rev. Lett. **63**, 1996 (1989).